

Lawrence Berkeley National Laboratory

LBL Publications

Title

Coupling gas purging with inorganic carbon supply to enhance biohydrogen production with *Clostridium thermocellum*

Permalink

<https://escholarship.org/uc/item/7j529283>

Authors

Kim, Changman

Wolf, Isaac

Dou, Chang

et al.

Publication Date

2023

DOI

10.1016/j.cej.2022.141028

Copyright Information

This work is made available under the terms of a Creative Commons Attribution License, available at <https://creativecommons.org/licenses/by/4.0/>

Peer reviewed

1 Date: Nov 5th, 2022

2 For submission to *Chemical Engineering Journal*

3

4 **Coupling gas purging with inorganic carbon supply to enhance**
5 **biohydrogen production with *Clostridium thermocellum***

6

7 **Changman Kim^{1,2}, Isaac Wolf¹, Chang Dou¹, Lauren Magnusson³, Pin-Ching Maness³,**
8 **Katherine J. Chou³, Steven Singer^{4,5}, Eric Sundstrom^{1,5,*}**

9

10 ¹ Advanced Biofuel and Bioproducts Process Development Unit, Lawrence Berkeley National
11 Laboratory, Emeryville, CA, 94608, USA

12 ² Department of Biotechnology and Bioengineering, Chonnam National University, Gwangju,
13 61186, Republic of Korea

14 ³ Biosciences Center, National Renewable Energy Laboratory, Golden, CO 80401, USA

15 ⁴ Joint BioEnergy Institute, 5885 Hollis street, 4th floor, Emeryville, CA, 94608, USA

16 ⁵ Biological System Engineering Division, Lawrence Berkeley National Laboratory, 1
17 Cyclotron Road, Berkeley, CA, 94702, USA

18

19

20 ***Corresponding author**

21 **Eric Sundstrom, PhD**

22 *Address:* Advanced Biofuel and Bioproducts Process Development Unit, Lawrence Berkeley
23 National Laboratory, Emeryville, CA, 94608, USA

24 *E-mail address:* esundstrom@lbl.gov

25

26 **Abstract**

27 *Clostridium thermocellum* is a desirable biocatalyst for biohydrogen production, with a native
28 ability to simultaneously saccharify cellulose and to metabolize released cellodextrins for
29 hydrogen production. During fermentation with *C. thermocellum*, partial pressures of two
30 gases - CO₂ and H₂ - are critical drivers of overall reaction kinetics. Biohydrogen production
31 is enhanced by maintaining a low hydrogen partial pressure, while high concentrations of
32 dissolved CO₂ promote microbial biomass synthesis. Our study evaluates the inherent trade-
33 offs between hydrogen stripping and inorganic carbon supply for optimized biohydrogen
34 synthesis. We find that nitrogen sparging at low flow rates increases hydrogen production
35 when compared with an equivalent nitrogen overlay, but that high rates of nitrogen sparging
36 inhibit cell growth and hydrogen production. Decreasing dissolved hydrogen partial pressure
37 via nitrogen sparging also lowers production of reduced metabolites, including lactate and
38 ethanol. To address potential stripping of inorganic carbon from the production medium, we
39 supplemented CO₂ to the sparging gas and co-optimized for gas flow rate and for the CO₂
40 fraction of the sparging gas. Total hydrogen production increased from 50 mmol·L⁻¹ in the
41 base condition, when the bioreactor was sparged with 0.1 LPM of pure nitrogen, to 181.3
42 mmol·L⁻¹ when sparged with 1.3 LPM of 33% CO₂, demonstrating that biohydrogen
43 production is highly sensitive to both parameters. Fine sensitivity of biohydrogen production
44 to sparging conditions highlights the critical importance of bioreactor design and operation to
45 achieve maximum H₂ removal without compromising inorganic carbon supply to bacterial
46 central metabolism.

47 **Keywords:** *Clostridium thermocellum*; Biohydrogen; Gas sparging; Avicel1.

48 **Introduction**

49 Biological hydrogen production is an intriguing technology for conversion of
50 complex organic waste streams into a renewable, dispatchable, and fungible energy carrier [1,
51 2]. Dark fermentation using lignocellulosic biomass is particularly appealing, as it allows for
52 cost-effective and profitable use of agricultural and forestry residue while avoiding the
53 adverse air pollution impacts associated with waste biomass combustion [3, 4]. Along with
54 hydrogen, dark fermentation produces a high-quality CO₂ stream that can be sold, sequestered,
55 or upgraded for further use, effectively decoupling energy release from biomass degradation
56 and the resulting CO₂ emissions [5, 6]. However, to make biohydrogen production
57 economically viable, conversion rates and yields must be improved, and these improvements
58 must be consistent with conditions found in larger-scale bioreactors. During bioreactor scale-
59 up, partial pressures of three gases (H₂, O₂, and CO₂) are critical factors impacting hydrogen
60 productivity, titer, and yield from cellulosic biomass [1].

61 Oxygen inhibits both native hydrogenase activity and the central metabolism of
62 hydrogen-producing anaerobic bacteria. To maintain anoxic conditions, most reactor
63 configurations apply nitrogen or argon to remove dissolved oxygen, with associated impacts
64 on dissolved hydrogen and carbon dioxide concentrations [7, 8]. High hydrogen partial
65 pressure can thermodynamically shift the reaction away from hydrogen generation and toward
66 hydrogen uptake [9, 10]. In such cases, hydrogenases can oxidize hydrogen by transferring
67 electrons to reduce cellular redox co-factors, including NAD⁺ and ferredoxin ([11]). At
68 present, two opposing ideas describe the impact of CO₂ partial pressure on biohydrogen
69 fermentations. *Park et al.* demonstrated that headspace CO₂ removal enhances secondary
70 autotrophic metabolism by acetogens in a mixed community of microorganisms [12], while
71 *Kim et al.* proposed CO₂ sparging as thermodynamically beneficial for H₂ production [13].

72 Bioconversion of lignocellulosic biomass can be typically viewed as a two-step
73 process: 1) the polysaccharides are broken down into monomeric sugars or soluble sugar
74 oligomers; 2) the soluble sugars are fermented and converted to the target products. In many
75 engineered and natural systems, mixed microbial cultures accomplish this dual role of
76 deconstruction and fermentation via division of labor. Although mixed cultures can
77 metabolize complex and recalcitrant lignocellulosic feedstocks, mixed culture approaches
78 often result in lower productivity of specific target products due to increased metabolic
79 complexity [3, 4]. In contrast to mixed microbial systems, the Gram-positive, thermophilic,
80 and obligate-anaerobic biocatalyst *Clostridium thermocellum* is capable of achieving biomass
81 conversion to products in pure culture, owing to its natural ability to produce cellulosomes:
82 multi-enzyme complexes bearing cellulase and xylanase enzymes highly effective in
83 depolymerizing cellulose and hemicellulose into their soluble hexose and pentose sugar
84 constituents. *C. thermocellum* can therefore hydrolyze and ferment complex cellulosic
85 biomass in one integrated process known as consolidated bioprocessing (CBP) [14]. This
86 process results in production of hydrogen, ethanol, and organic acids with acetate typically
87 produced in greater quantities than lactate and formate [15, 16]. *C. thermocellum* has three
88 [Fe-Fe] hydrogenases and one ferredoxin-dependent [NiFe] hydrogenase which are
89 presumably correlated to anaerobic redox metabolism [17, 18]. Previous reports have
90 successfully demonstrated biohydrogen production from cellulosic biomass (avicel) and
91 xylose using *C. thermocellum* [19]. However, further development is required to improve
92 both hydrogen yield and productivity under industrially relevant conditions [15, 16].

93 Active CO₂ fixation metabolism during cellulose assimilation has been reported in
94 *C. thermocellum*, a unique feature of this organism [20]. Although the relationship between

95 CO₂ metabolism and hydrogen production was not clearly elucidated, Xiong et al.
96 demonstrated that bicarbonate addition can improve not only carbon recovery, but also
97 essential cell physiological activities including amino acid synthesis and cell growth.
98 Therefore, while enhanced hydrogen removal via gas stripping may boost the hydrogen
99 production metabolism, it may simultaneously strip CO₂ from the solution, negatively
100 affecting amino acid synthesis and cell growth.

101 In this study, we aim to develop gas sparging strategies for improved biohydrogen
102 fermentation from cellulose-based biomass by *C. thermocellum* by effectively balancing
103 hydrogen removal and CO₂ supply. We focus on examining the potential trade-off between N₂
104 sparging rates and CO₂ partial pressures, and their relative impacts on cellular metabolism,
105 cell biomass production, and hydrogen production. In addition, we evaluate these parameters
106 in fermentations with high concentrations of cellulose (45 g/L), creating metabolite profiles,
107 mixing conditions, and culture viscosities representative of high-intensity biohydrogen
108 production conditions. Taken together, we show that the effects of H₂ removal and inorganic
109 carbon supply on the bacteria are coupled, and we demonstrate that engineering interventions
110 -including CO₂ supplementation during gas stripping - can substantially improve hydrogen
111 production in high-solids fermentations without compromising *C. thermocellum* central
112 metabolism.

113

114 **2. Materials and methods**

115 **2.1. Strain and materials**

116 *Clostridium thermocellum* KJC315 (a DSM1313 derived strain, Δhpt) was provided

117 by NREL [20]. In this study, two different media were used for microbial cell growth and
118 biohydrogen production. CTFUD rich media includes (per liter in D.W.): 3 g $\text{Na}_3\text{C}_6\text{H}_5\text{O}_7\cdot\text{H}_2\text{O}$,
119 1.3 g $(\text{NH}_4)_2\text{SO}_4$, 1.5 g KH_2PO_4 , 0.13 g $\text{CaCl}_2\cdot\text{H}_2\text{O}$, 2.6 g $\text{MgCl}_2\cdot 6\text{H}_2\text{O}$, 1 mg $\text{FeSO}_4\cdot 7\text{H}_2\text{O}$,
120 11.56 g MOPS sodium salt, 0.5 g L-cysteine HCl, 5g cellobiose, 4.5 g yeast extract, 0.5 mL of
121 1000x resazurin solution. MTC contains the following components (per liter in D.W.): 5 g
122 MOPS sodium salt, 2 g $\text{Na}_3\text{C}_6\text{H}_5\text{O}_7\cdot\text{H}_2\text{O}$, 1 g K_2HPO_4 , 1.25 g $\text{C}_6\text{H}_8\text{O}_7\cdot\text{H}_2\text{O}$, 1 g Na_2SO_4 , 2.5 g
123 NaHCO_3 , 1.5 g NH_4Cl , 2 g urea, 1 g, $\text{MgCl}_2\cdot 6\text{H}_2\text{O}$, 0.2 g $\text{CaCl}_2\cdot 2\text{H}_2\text{O}$, 1 mg $\text{FeSO}_4\cdot 7\text{H}_2\text{O}$, 1 g
124 L-cysteine HCl, 20 mg pyridoxamine dihydrochloride, 4 mg PABA, 2 mg D-biotin, 2 mg
125 vitamin B₁₂, 0.5 mL of pre-made resazurin solution (44 mM). Prior to inoculation, both
126 medium was adjusted to pH 7.0 using 2 N NaOH and 10 % H_2SO_4 . MTC media was
127 supplemented with 5 g/L D-(+)-Cellobiose. MTC media was also used in all bioreactor
128 fermentations, and was supplemented with 30 g/L of Avicel PH-101 (~ 50 μm particle size,
129 Sigma Aldrich, USA) ,or 20 g/L of D-(+)-Cellobiose as specified in the results section.
130 CTFUD rich media was used for bacteria storage in -80 °C, growth, and reactivation of seed 1
131 cultures. For pre-culture 2 and main fermentation, MTC media was applied.

132

133 **2.2. Bioreactor operation**

134 Seed culture cultivation was performed using two consecutive seed trains at 10 mL
135 and 50 mL culture volume (in 20- and 125-ml serum bottles, respectively) incubated in a
136 rotary shaker at 60 °C and 150 rpm for 24 h. Initial seed cultures were reactivated from frozen
137 stock in CTFUD rich media, before transferring to a second seed cultivated in MTC media
138 containing 5 g/L D-(+)-Cellobiose. Main cultivation was performed with 0.95 L MTC media

139 and 0.05 L inoculum in 2 L jacketed BIOSTAT® B (Sartorius AG., Goettingen, Germany)
140 benchtop bioreactors with dual Rushton impellers and constant gas flow regulator. Process
141 parameters were 60 °C and 100 rpm agitation with pH controlled at 7.0 using 2 M NaOH. A
142 default flow rate of 0.1 liters per minute (LPM) was utilized for nitrogen, carbon dioxide and
143 mixed gases unless otherwise specified. All bioreactors were sparged with a ring sparger
144 sitting below the lowest impeller and containing 14 holes, with each hole 1mm in diameter.
145 Gases were supplied either directly to the gas headspace of the bioreactor (overlay), or via
146 sparging into liquid culture (sparged). Manual 5 mL samples were taken throughout the
147 cultivation and stored at 4 °C for further analysis.

148 **2.3. Analysis**

149 The concentrations of sugars and other byproducts (e.g., formic acid, lactic acid, acetic acid,
150 ethanol, and glycerol) in the fermentation samples were quantified using a high-performance
151 liquid chromatography (HPLC) system (Ultimate 3000, Thermo Fisher Scientific, Waltham,
152 MA) equipped with a refractive index detector and an Aminex HPX-87H column (Bio-Rad,
153 300 × 7.8 mm, Hercules, CA, USA). The mobile phase (4 mM of H₂SO₄ solution) flowed at a
154 rate of 0.4 mL/min and the column oven temperature was set at 40 °C for HPLC operation.
155 The off-gas of the fermentation was monitored using a magnetic sector MS analyzer (Prima
156 BT Bench Top Process Mass Spectrometer, Thermo Fisher Scientific, Waltham, MA) by
157 which the concentrations of N₂, CO₂, H₂, O₂ were monitored in real time. H₂ production rates
158 were quantified by comparison with known flow rates of inert N₂ supplied to the bioreactor
159 with the following equation.

160
$$H_2 \text{ production rate (LPM)} = \frac{N_2 \text{ flow rate (LPM)} \times \text{Measured } H_2 \text{ concentration (\%)}}{\text{Measured } N_2 \text{ concentration (\%)}}$$

161 All analyses were conducted in duplicate or triplicate and presented as the average value.

162

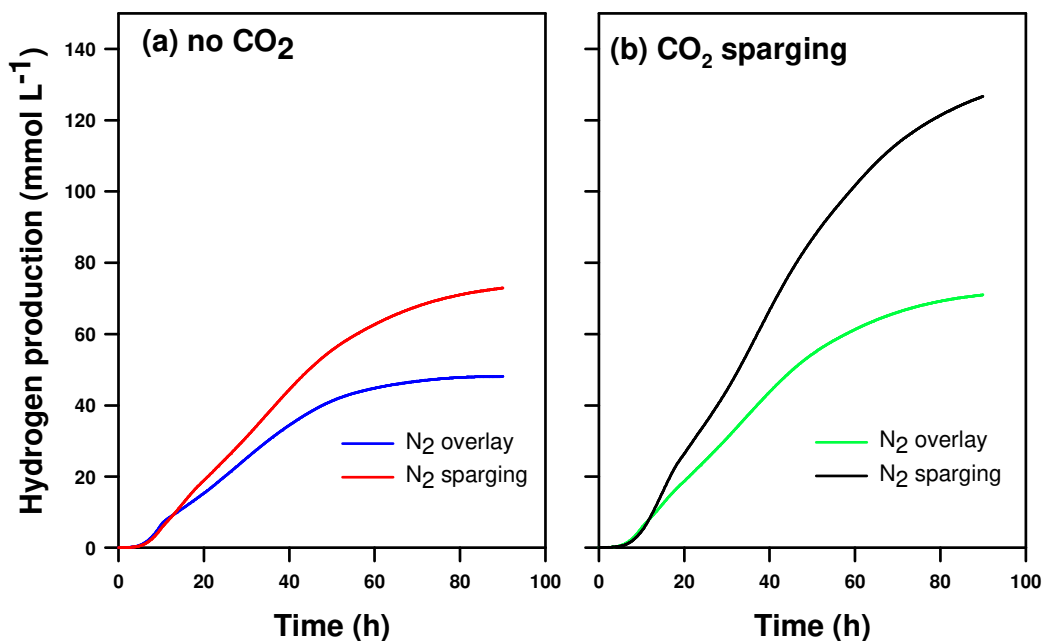
163 **3. Results and discussions**

164 **3.1. Gas purging strategies in biohydrogen production**

165 Strict anaerobic conditions are required for optimal *C. thermocellum* growth, and
166 these conditions are typically maintained by continuous purging with biologically non-
167 reactive gases, including nitrogen and argon. In agitated bioreactor fermentations there are
168 two potential modes of gas purging: gas overlay with inert gas supplied to the reactor
169 headspace and gas sparging with inert gas sparged directly into the liquid culture. To evaluate
170 the differences in *C. thermocellum* metabolic response to these strategies, bioreactors were
171 operated with either overlay nitrogen or sparged nitrogen supplied at 0.1 LPM into 1 L of
172 liquid culture for comparison. Data from [Fig. 1 \(a\)](#) shows hydrogen production profiles
173 between overlay and sparged bioreactors purged with 0.1 LPM of nitrogen and supplied with
174 30 g/L of avicel. Under these conditions, sparged bioreactors produced more hydrogen (72.9
175 mmol · L⁻¹) compared with overlay bioreactors (48.1 mmol · L⁻¹). Generally, nitrogen
176 sparging improves the thermodynamic preference for biohydrogen production by decreasing
177 both the hydrogen partial pressure in the reactor headspace and by reducing the dissolved
178 hydrogen concentration in media [8, 21]. In this study, both overlay and sparging reactors
179 should have similar headspace hydrogen partial pressure because the continuous purging gas
180 diluted the produced hydrogen gas (maintained below 2 % in both reactors), even if gas

181 bubbling increased the gas-liquid interface area. However, because nitrogen sparging can
182 extrude dissolved hydrogen in the media, sparged cultures are likely subjected to lower
183 hydrogen partial pressures in the aqueous phase.

184



185

186 **Figure 1.** Hydrogen production profiles (a) without CO₂ and (b) with CO₂ sparging between
 187 N₂ sparging and overlay reactors, at a flow rate of 0.1 LPM (n = 2), using 30 g/L avicel as a
 188 substrate.

189 To determine the effects of nitrogen sparging on dissolved hydrogen in the media,
 190 an abiotic experiment was conducted, confirming elevated hydrogen stripping rates in the
 191 nitrogen sparging condition (Fig S1). According to the results, direct sparging accelerated
 192 hydrogen stripping when compared to overlay purging. Therefore, in isolation, relatively low
 193 dissolved hydrogen concentrations tend to boost *C. thermocellum* biohydrogen generation.

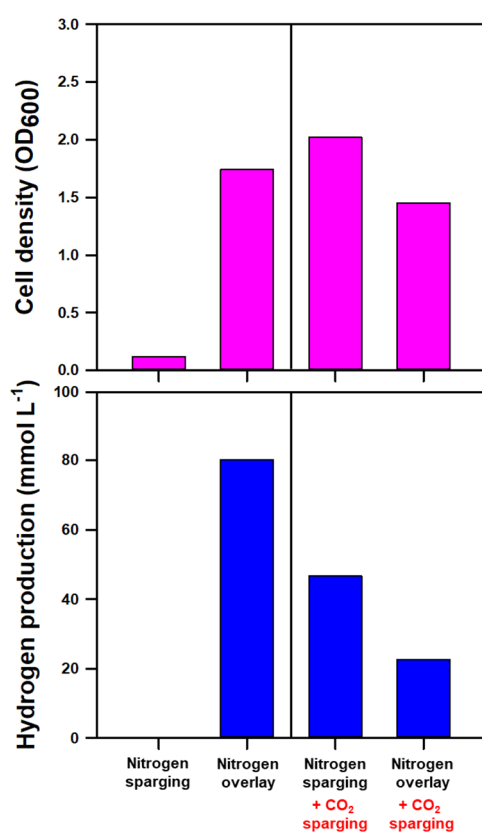
194 Xiong et al. demonstrate that the addition of sodium bicarbonate correlates with a
 195 higher *C. thermocellum* cell biomass when using cellobiose as the carbon source [20]. To
 196 evaluate the impact of sparging conditions on inorganic carbon availability, abiotic bioreactor
 197 operations with 0.1 LPM nitrogen sparging were examined in combination with the addition
 198 of a 47.6 mmol sodium bicarbonate bolus. Fig S2 depicts CO₂ release profiles in abiotic

199 reactors, with approximately 85 % of inorganic carbon (40.7 mmol) stripped out within 8
200 hours during the reactor deoxygenating and pre-conditioning stage. The water solubility of
201 CO₂ is only 0.58 g/L under the *C. thermocellum* fermentation condition (1 atm at 60 °C).
202 MTC media contains 2.2 g/L of HCO₃⁻ (2.5 g/L of NaHCO₃); however theoretically around
203 1.5 g/L of bicarbonate was discharged from the media via gas sparging prior to inoculation,
204 leaving only 0.5–0.7 g/L of dissolved CO₂ species at the time of inoculation.

205 To compensate for this gas stripping effect and provide a more stable supply of
206 inorganic carbon, two additional conditions were evaluated in which pure nitrogen was
207 substituted with a mixed purging gas containing approximately 33% CO₂ (0.033 LPM of 100 %
208 CO₂) and 67% N₂ (0.067 LPM of 100 % N₂), ensuring constant partial pressure of CO₂
209 throughout the fermentation. In these reactors, CO₂ supplementation resulted in 1.7 and 1.5-
210 fold higher hydrogen production (126.7 and 71.0 mmol in N₂ sparging and overlay reactor,
211 respectively) (Fig 1(b)), compared with reactors receiving pure N₂ (Fig 1 (a)).

212 Cell growth experiments were also conducted to determine the effects of gas
213 purging using D-(+)-cellobiose as a substrate instead of Avicel, as 30 g/L Avicel media
214 solution is too milky for effective OD measurement (Fig 2). Pure nitrogen sparging
215 significantly inhibited bacterial growth at a flow rate of 0.1 LPM. Mixed N₂ and CO₂ sparging
216 enabled *C. thermocellum* to fully utilize cellobiose in both the 0.1 and 0.2 LPM reactors.
217 Nitrogen overlay resulted higher cell growth but lower hydrogen production, because
218 dissolved CO₂ and H₂ could be converted to biomass. Additional supply of CO₂ in the 0.1
219 LPM overlay reactor presented additional inorganic carbon uptake due to the abundant CO₂
220 species in the media. These experiments confirm the need for a consistent supply of inorganic
221 carbon in *C. thermocellum* biohydrogen production, particularly when CO₂ produced during

222 cellulose metabolism is rapidly stripped from the solution as part of a hydrogen removal
223 strategy. Notably, while $72.9 \text{ mmol} \cdot \text{L}^{-1}$ hydrogen production was observed with 0.1 LPM
224 pure nitrogen sparging in the avicel condition presented in figure 1, no production at all was
225 observed under equivalent conditions with cellobiose feedstock. This variability is likely
226 attributed to the high viscosity of the avicel-containing cultivation medium, which dampens
227 mixing and liquid-gas mass transfer, diminishing the rate of CO_2 stripping from the system.

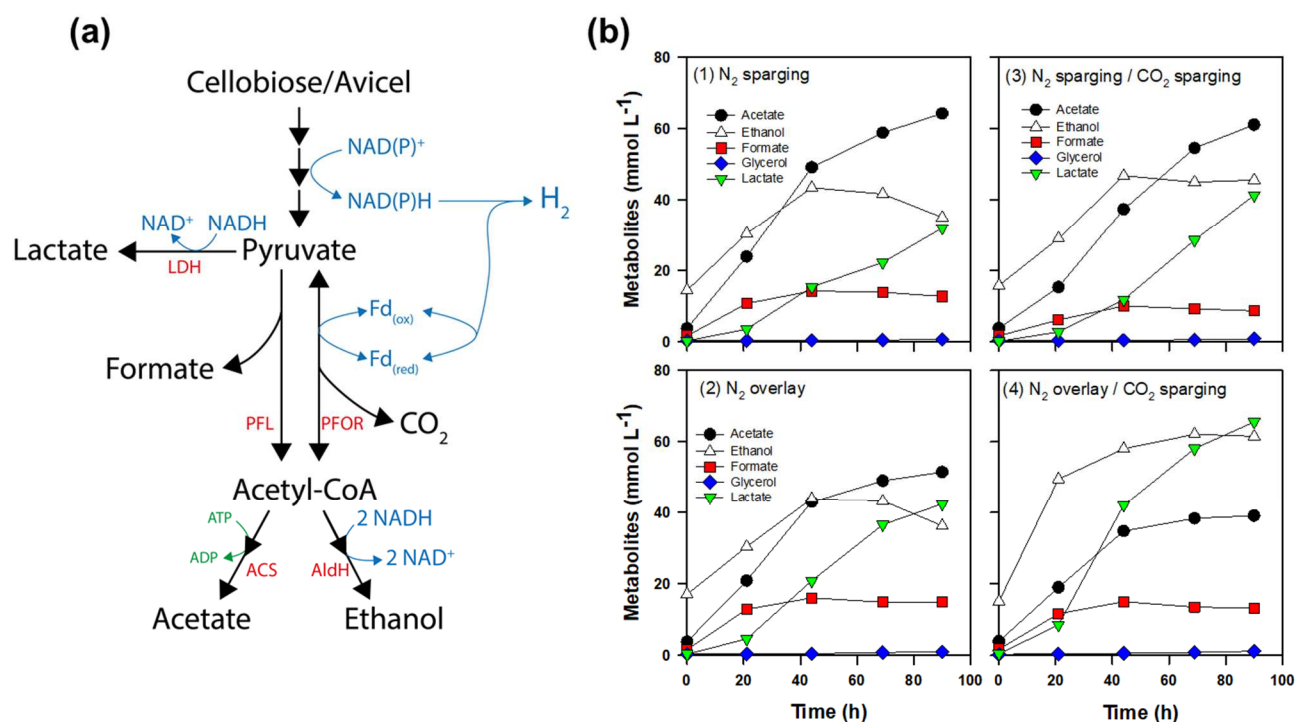


228
229 **Figure 2.** Cell density and hydrogen productions for *C. thermocellum* after 48 hours of
230 growth using cellobiose (5 g/L) as a substrate. Overlay and sparged gases were supplied at a
231 total flow rate of 0.1 LPM.

232

233 **3.2. Metabolic characterization of *C. thermocellum* hydrogen production**

234 To further understand the effect of gas purging strategies on bacterial metabolism
 235 during Avicel fermentation, metabolites were analyzed from four different bioreactor
 236 configurations: 1) N₂ sparging, 2) N₂ overlay, 3) N₂ and CO₂ sparging and 4) N₂ overlay and
 237 CO₂ sparging. N₂ sparging reactors (conditions 1 and 3) should exhibit enhanced hydrogen
 238 removal rates when compared with N₂ overlay reactors (conditions 2 and 4). CO₂ sparging
 239 reactors (3 and 4) contained higher concentrations of dissolved CO₂ when compared with
 240 non-CO₂ sparging reactors (1 and 2). Fig 3b and Table 1 present the production of key
 241 fermentation byproducts and the metabolic pathways leading to their production in *C.*
 242 *thermocellum*.



243
 244 **Figure 3.** (a) Metabolic pathway from cellobiose/Avicel and (b) metabolites profiles of the

245 different gas purging reactors

246 **Table 1.** Comparison of metabolites produced when utilizing variable gas purging strategies

Purging gas		Metabolites (mmol L ⁻¹)					H ₂ /Acetate (mol/mol)
N ₂	CO ₂	H ₂	Acetate	Ethanol	Formate	Lactate	
Sparging	-	72.9	64.3	35.1	13.1	32.4	1.1
Overlay	-	48.1	61.1	45.6	8.9	41.8	0.8
Sparging	Sparging	126.7	61.5	36.3	15.3	42.9	2.1
Overlay	Sparging	71	39.1	61.6	13.5	66.3	1.8

247

248 Hydrogen production is an “electron sink” for *C. thermocellum* metabolism when
249 balancing the cellular redox state [22, 23]. Hydrogen stripped from the solution by nitrogen
250 sparging effectively decreases the concentration of dissolved hydrogen in the media, shifting
251 the thermodynamic equilibrium to favor additional hydrogen production. This process may
252 therefore lead to a shift of metabolic carbon flux towards non-reducing pathways. As a result,
253 N₂ sparged reactors produced fewer reduced metabolites, including lactate and ethanol, when
254 compared to the N₂-overlay reactors in which additional CO₂ was supplied via sparging.

255 Pyruvate ferredoxin oxidoreductase (PFOR) can catalyze the reductive
256 carboxylation of CO₂ and incorporate CO₂ to produce pyruvate from acetyl-CoA, even under
257 cellulose-degrading conditions [20]. This reversed PFOR-driven CO₂ uptake pathway may be
258 crucial for the biosynthesis of serine, methionine, and cell biomass via C1 metabolism.
259 Continuous supply of CO₂ may increase the carbon flux toward pyruvate synthesis, further led
260 to lactate production as overflow metabolism. This is consistent with higher lactate
261 production in the CO₂ sparging reactors. Our data is also consistent in showing that
262 production of lactate outcompetes production of ethanol during CO₂ sparging as acetyl-CoA,
263 a precursor to form ethanol, was depleted to form pyruvate and subsequently routed to lactate
264 instead.

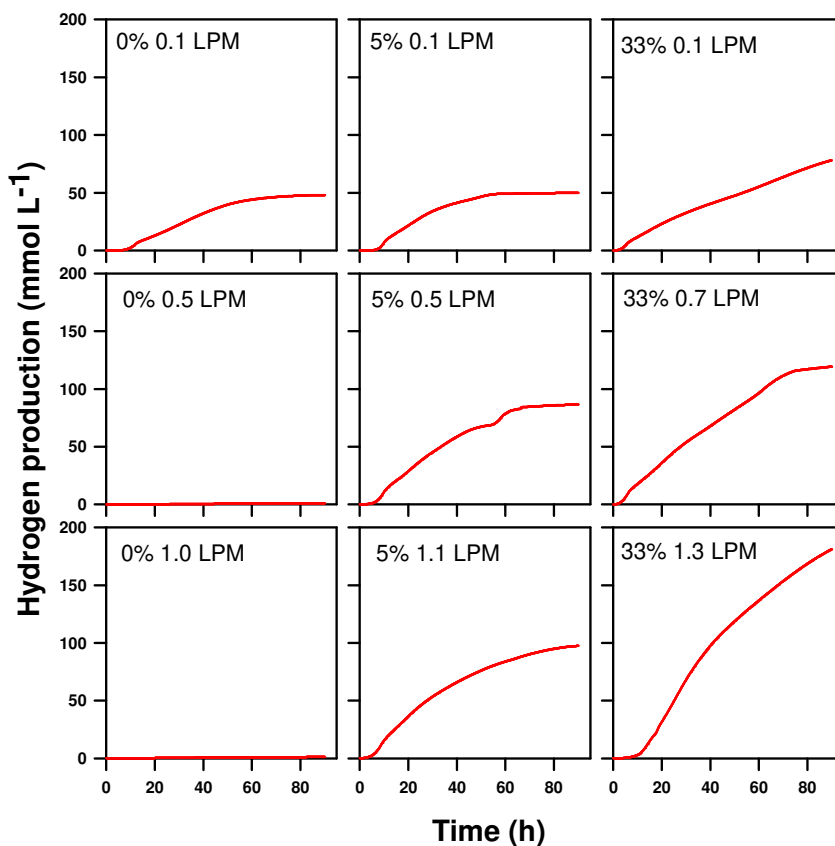
265 Acetate is regarded as a primary byproduct in dark fermentation, often used to
266 assess the H₂/Acetate ratio [24]. The theoretical equation ($C_6H_{12}O_6 + 2 H_2O \rightarrow 2 CH_3COOH$
267 $+ 2 CO_2 + 4 H_2$) implies the ideal maximum ratio between hydrogen and acetate as 2.
268 However, the true value varies with bacterial species and process conditions. Shen et al.
269 proposed that relatively higher H₂/Acetate ratios could denote acetate oxidation or acetyl-CoA
270 consumption, including CO₂ fixation by PFOR [24]. Formation of the reduced metabolites

271 lactate and ethanol, utilizing NADH as a co-factor, tends to decrease the H₂/Acetate ratio due
272 to lowered hydrogen synthesis. When comparing replicates with CO₂ sparging, *C.*
273 *thermocellum* with an N₂ overlay synthesized comparatively higher concentrations of lactate
274 and lower concentrations of acetate, likely due to higher concentrations of dissolved hydrogen.

275

276 **3.3. Optimization of gas sparging strategies**

277 To further optimize biohydrogen production in bioreactor fermentations and deduce
278 the interaction between hydrogen removal and CO₂ supply, we explored a variety of gas
279 sparging rates and gas compositions in a full-factorial experimental design illustrated in [Fig 4](#).
280 These experiments were conducted with three sparging rates (0.1, 0.5, and 1.0 LPM for
281 nitrogen gas) and three CO₂ concentrations (0, 5, and 33%), using modified MTC media
282 containing lower concentration of vitamins (30% of the full recipe).



283

284 **Figure 4.** Hydrogen production profiles during Avicel (30 g/L) fermentation for variable gas
 285 sparging conditions

286 Among 100% nitrogen sparging reactors, significant hydrogen production was only
 287 identified at 0.1 LPM (48.1 mmol·L⁻¹) (Fig 4). Remarkably, higher sparging rates with 100%
 288 nitrogen (0.5 and 1.0 LPM), resulted in no biohydrogen production nor Avicel metabolism
 289 over 24 hours monitoring. As demonstrated in Fig S2, a higher nitrogen sparging rate
 290 accelerates the CO₂ release rate. Thus, the media in these conditions may not maintain
 291 sufficient inorganic carbon for essential microbial metabolism, highlighting the reliance of *C.*
 292 *thermocellum* on CO₂ for growth on organic substrates. Hydrogen production, with a small
 293 amount (~ 5% v/v) of CO₂ sparging, was measured at 50.0, 86.6 and 97.4 mmol·L⁻¹ in 0.1, 0.5
 294 and 1.1 LPM reactors, respectively. In contrast to the 100% nitrogen sparging condition, even

295 small amounts of CO₂ during gas sparging provided a sufficient inorganic carbon source,
296 allowing *C. thermocellum* to generate the biomass required to metabolize Avicel and generate
297 hydrogen. Higher concentration of CO₂ in the gas sparging stream resulted in further
298 improvements to hydrogen production titers when compared with no/low concentration of
299 CO₂ sparging reactors (78.2, 119.4 and 181.3 mmol·L⁻¹ with 0.1, 0.5 and 1.0 LPM,
300 respectively). As a result, we conclude that both high CO₂ partial pressures and high gas
301 stripping rates are essential to maximize biohydrogen production as illustrated in Fig 3 (b).
302 Notably, hydrogen production with the 0.1 LPM sparging rate was similar until early- to mid-
303 stage production (45 hours) despite variable sparging gas compositions (36.3, 44.0 and 44.1
304 mmol·L⁻¹ with 0, 5 and 33 % CO₂, respectively). This implies that addition of CO₂ gas at low
305 sparging rates primarily serves to prolong productivity into the mid- to late- stages of
306 fermentation. With lower sparging rates, biogenically released CO₂ appears sufficient to
307 maintain central metabolic activity in the early stages of production. Supplemental CO₂ may
308 prolong culture viability in later stages as metabolic activity slows, with an associated
309 reduction in the availability of biogenic inorganic carbon.

310 Metabolite production profiles under variable gas sparging regimes are shown in
311 Fig S3. To understand the correlation between gas sparging rate, CO₂ concentration,
312 metabolites, and hydrogen production, Pearson's correlation analysis was conducted (Fig S4).
313 The results of this statistical analysis indicate that CO₂ concentration, hydrogen production,
314 acetate production, and formate production have a positive and significant correlation ($P >$
315 0.7). Pyruvate formate lyase is the core enzyme for the conversion of pyruvate to acetyl-CoA
316 and formate in the anaerobic cellulosic metabolism of *C. thermocellum*. The conversion of
317 acetyl-CoA to acetate is a key ATP-synthesis step, which does not affect the cellular redox

318 state. Relatively optimized conditions, including sufficient gas sparging and sufficient
319 inorganic carbon source, allowed *C. thermocellum* to metabolize Avicel for synthesis of
320 acetate and formate. Similarly, lactate production was significantly correlated with both H₂
321 production and CO₂ concentration ($0.3 < P < 0.7$). Sparging rates have a moderate level of
322 correlation with hydrogen production ($P = 0.4$) because of out-range results from non-
323 hydrogen productive reactors (0.5 and 1.0 LPM with 100 % nitrogen). This result further
324 illustrates that sparging impacts cannot be considered in isolation, without considering
325 inorganic carbon availability.

326 The results of *C. thermocellum* fermentation with 100% CO₂ sparging were
327 summarized in Fig S5. After 24 h, the hydrogen production rates of the 100% CO₂ sparging
328 reactors (56.0, 56.4, and 43.7 mmol·L⁻¹·day⁻¹ for 0.1, 0.5, and 1.0 LPM, respectively) were
329 significantly higher than those of the mixed gas sparging reactors (27.3, 43.7, and 45.7
330 mmol·L⁻¹·day⁻¹ for 0.1, 0.6, and 1.3 LPM, respectively). However, hydrogen production
331 dropped after 1 day for all 100% CO₂ sparging reactors. A small amount of reduced
332 ferredoxin remained may have still been available to serve as an electron donor for hydrogen
333 production owing to the re-oxidation of ferredoxin catalyzed by reversed PFOR. Metabolite
334 profiles presented significantly higher concentrations of formate within 1 day, as shown in Fig
335 S5. This implies that a higher concentration of CO₂ sparging triggers the reverse reaction of
336 PFOR, resulting in overflow metabolism. Oversaturated CO₂-based metabolic interruption is
337 generally acceptable in various bacteria species [25]. To prevent supersaturation of CO₂ in the
338 media, mixed gas should therefore be used to achieve optimal biohydrogen production in *C.*
339 *thermocellum*. While this approach is highly effective at a bench scale, further scale-up of
340 biohydrogen production will likely require the development of alternative gas stripping

341 methods to avoid energy costs for sparging and to maximize hydrogen concentration in the
342 off-gas. These approaches could potentially include vacuum or membrane-based methods
343 [26], to avoid the high costs associated with gas sparging and downstream separation of
344 gaseous products. Such strategies must be optimized to maintain adequate inorganic carbon
345 while minimizing both H₂ partial pressures and dilution of H₂ in the output gas stream.

346

347 **4. Conclusion**

348 In this study, we developed gas sparging strategies for optimal cellulosic
349 biohydrogen production using *C. thermocellum* in 1 L bioreactors. Nitrogen sparging
350 enhanced hydrogen removal and overall hydrogen productivity when compared to a nitrogen
351 overlay. Continuous supply of inorganic carbon by CO₂ sparging combined with high overall
352 gas sparging rates increased hydrogen productivity from 50 mmol·L⁻¹ in the nitrogen sparging
353 base condition to 181.3 mmol·L⁻¹ when supplied with a high flow rate of 33% CO₂. This
354 result demonstrates that a co-optimized sparging rate and CO₂ concentration can achieve rapid
355 hydrogen removal while preserving inorganic carbon supplies, thereby maximizing
356 biohydrogen generation.

357

358 **5. Acknowledgement**

359 This work was in part authored by the Lawrence Berkeley National Laboratory and National
360 Renewable Energy Laboratory (NREL), operated by Alliance for Sustainable Energy, LLC,
361 for the U.S. Department of Energy (DOE) under Contract No. DE-AC36-08GO28308.
362 Funding was provided by U.S. Department of Energy Office of Energy Efficiency Renewable

363 Energy Hydrogen and Fuel Cell Technologies Office. The views expressed in the article do
364 not necessarily represent the views of the DOE or the U.S. Government. The U.S.
365 Government retains and the publisher, by accepting the article for publication, acknowledges
366 that the U.S. Government retains a nonexclusive, paid-up, irrevocable, worldwide license to
367 publish or reproduce the published form of this work, or allow others to do so, for U.S.
368 Government purposes. Authors declare no competing interests.

369

370 **6. References**

371 [1] A. Ghimire, L. Frunzo, F. Pirozzi, E. Trably, R. Escudie, P.N. Lens, G. Esposito, A review
372 on dark fermentative biohydrogen production from organic biomass: process parameters and
373 use of by-products, *Applied Energy* 144 (2015) 73-95.

374 [2] J.-H. Jung, Y.-B. Sim, J.-H. Park, A. Pandey, S.-H. Kim, Novel dynamic membrane,
375 metabolic flux balance and PICRUSt analysis for high-rate biohydrogen production at various
376 substrate concentrations, *Chemical Engineering Journal* (2020) 127685.

377 [3] W. Han, Y.Y. Hu, S.Y. Li, F.F. Li, J.H. Tang, Biohydrogen production from waste bread
378 in a continuous stirred tank reactor: A techno-economic analysis, *Bioresource technology* 221
379 (2016) 318-323.

380 [4] Y.-C. Li, Y.-F. Liu, C.-Y. Chu, P.-L. Chang, C.-W. Hsu, P.-J. Lin, S.-Y. Wu, Techno-
381 economic evaluation of biohydrogen production from wastewater and agricultural waste,
382 *International journal of hydrogen energy* 37(20) (2012) 15704-15710.

383 [5] J.-H. Lu, C. Chen, C. Huang, H. Zhuang, S.-Y. Leu, D.-J. Lee, Dark fermentation
384 production of volatile fatty acids from glucose with biochar amended biological consortium,
385 *Bioresource technology* 303 (2020) 122921.

- 386 [6] A. Chalima, A. Hatzidaki, A. Karnaouri, E. Topakas, Integration of a dark fermentation
387 effluent in a microalgal-based biorefinery for the production of high-added value omega-3
388 fatty acids, *Applied Energy* 241 (2019) 130-138.
- 389 [7] P.T. Sekoai, K.O. Yoro, M.O. Daramola, Effect of nitrogen gas sparging on dark
390 fermentative biohydrogen production using suspended and immobilized cells of anaerobic
391 mixed bacteria from potato waste, *Biofuels* 9(5) (2018) 595-604.
- 392 [8] O. Mizuno, R. Dinsdale, F.R. Hawkes, D.L. Hawkes, T. Noike, Enhancement of hydrogen
393 production from glucose by nitrogen gas sparging, *Bioresource technology* 73(1) (2000) 59-
394 65.
- 395 [9] L. Beckers, J. Masset, C. Hamilton, F. Delvigne, D. Toye, M. Crine, P. Thonart, S.
396 Hiligsmann, Investigation of the links between mass transfer conditions, dissolved hydrogen
397 concentration and biohydrogen production by the pure strain *Clostridium butyricum*
398 CWBI1009, *Biochemical Engineering Journal* 98 (2015) 18-28.
- 399 [10] B. Laurent, H. Serge, M. Julien, H. Christopher, T. Philippe, Effects of hydrogen partial
400 pressure on fermentative biohydrogen production by a chemotropic *Clostridium* bacterium in
401 a new horizontal rotating cylinder reactor, *Energy procedia* 29 (2012) 34-41.
- 402 [11] Y. Zheng, J. Kahnt, I.H. Kwon, R.I. Mackie, R.K. Thauer, Hydrogen formation and its
403 regulation in *Ruminococcus albus*: involvement of an electron-bifurcating [FeFe]-
404 hydrogenase, of a non-electron-bifurcating [FeFe]-hydrogenase, and of a putative hydrogen-
405 sensing [FeFe]-hydrogenase, *Journal of bacteriology* 196(22) (2014) 3840-3852.
- 406 [12] W. Park, S.H. Hyun, S.-E. Oh, B.E. Logan, I.S. Kim, Removal of headspace CO₂
407 increases biological hydrogen production, *Environmental science & technology* 39(12) (2005)
408 4416-4420.

- 409 [13] D.-H. Kim, H.-S. Shin, S.-H. Kim, Enhanced H₂ fermentation of organic waste by CO₂
410 sparging, *International journal of hydrogen energy* 37(20) (2012) 15563-15568.
- 411 [14] L.R. Lynd, C.E. Wyman, T.U. Gerngross, Biocommodity engineering, *Biotechnology*
412 *progress* 15(5) (1999) 777-793.
- 413 [15] D.B. Levin, R. Islam, N. Cicek, R. Sparling, Hydrogen production by *Clostridium*
414 *thermocellum* 27405 from cellulosic biomass substrates, *International Journal of Hydrogen*
415 *Energy* 31(11) (2006) 1496-1503.
- 416 [16] Q.-Q. Tian, L. Liang, M.-J. Zhu, Enhanced biohydrogen production from sugarcane
417 bagasse by *Clostridium thermocellum* supplemented with CaCO₃, *Bioresource Technology*
418 197 (2015) 422-428.
- 419 [17] H.-F. Li, B.L. Knutson, S.E. Nokes, B.C. Lynn, M.D. Flythe, Metabolic control of
420 *Clostridium thermocellum* via inhibition of hydrogenase activity and the glucose transport
421 rate, *Applied microbiology and biotechnology* 93(4) (2012) 1777-1784.
- 422 [18] T. Rydzak, P.D. McQueen, O.V. Krokhin, V. Spicer, P. Ezzati, R.C. Dwivedi, D.
423 Shamshurin, D.B. Levin, J.A. Wilkins, R. Sparling, Proteomic analysis of *Clostridium*
424 *thermocellum* core metabolism: relative protein expression profiles and growth phase-
425 dependent changes in protein expression, *BMC microbiology* 12(1) (2012) 1-18.
- 426 [19] W. Xiong, L.H. Reyes, W.E. Michener, P.C. Maness, K.J. Chou, Engineering cellulolytic
427 bacterium *Clostridium thermocellum* to co-ferment cellulose-and hemicellulose-derived
428 sugars simultaneously, *Biotechnology and bioengineering* 115(7) (2018) 1755-1763.
- 429 [20] W. Xiong, P.P. Lin, L. Magnusson, L. Warner, J.C. Liao, P.-C. Maness, K.J. Chou, CO₂-
430 fixing one-carbon metabolism in a cellulose-degrading bacterium *Clostridium thermocellum*,
431 *Proceedings of the National Academy of Sciences* 113(46) (2016) 13180-13185.

- 432 [21] D.-H. Kim, S.-K. Han, S.-H. Kim, H.-S. Shin, Effect of gas sparging on continuous
433 fermentative hydrogen production, *International Journal of Hydrogen Energy* 31(15) (2006)
434 2158-2169.
- 435 [22] H.-S. Lee, W.F. Vermaas, B.E. Rittmann, Biological hydrogen production: prospects and
436 challenges, *Trends in biotechnology* 28(5) (2010) 262-271.
- 437 [23] K.J. Chou, W. Xiong, L. Magnusson, M. Seibert, P.-C. Maness, *Renewable Hydrogen*
438 *From Biomass Fermentation*, (2020).
- 439 [24] N. Shen, F. Zhang, X.-N. Song, Y.-S. Wang, R.J. Zeng, Why is the ratio of H₂/acetate
440 over 2 in glucose fermentation by *Caldicellulosiruptor saccharolyticus*?, *International journal*
441 *of hydrogen energy* 38(26) (2013) 11241-11247.
- 442 [25] K.C. Peet, A.J. Freedman, H.H. Hernandez, V. Britto, C. Boreham, J.B. Ajo-Franklin,
443 J.R. Thompson, Microbial growth under supercritical CO₂, *Applied and environmental*
444 *microbiology* 81(8) (2015) 2881-2892.
- 445 [26] S. Singer, L. Magnusson, D. Hou, J. Lo, P.-C. Maness, Z.J. Ren, Anaerobic membrane
446 gas extraction facilitates thermophilic hydrogen production from *Clostridium thermocellum*,
447 *Environmental Science: Water Research & Technology* 4(11) (2018) 1771-1782.

448

449

Graphical abstract

